
Paper 2

Tormod Skauge, Iztok Turel and Einar Sletten.

"Interaction between ciprofloxacin and DNA mediated by Mg^{2+}-ions"

Inorganica Chimica Acta, 2002, 339, 239-247.

ELSEVIER

Inorganica Chimica Acta 339 (2002) 239–247

Inorganica Chimica Acta

www.elsevier.com/locate/ica

Interaction between ciprofloxacin and DNA mediated by Mg^{2+}-ions

T. Skauge [a], I. Turel [b], Einar Sletten [a,*]

[a] Department of Chemistry, University of Bergen, Allegt.41, N-5007 Bergen, Norway
[b] Faculty of Chemistry and Chemical Technology, University of Ljubljana, Aškerceva 5, 1000 Ljubljana, Slovenia

Received 9 November 2001; accepted 28 January 2002

Dedicated in honor of Professor Helmut Sigel

Abstract

The oligonucleotide duplex $d(C_1C_2T_3C_4G_5C_6T_7C_8T_9C_{10})\cdot d(G_{11}A_{12}G_{13}A_{14}G_{15}C_{16}G_{17}A_{18}G_{19}G_{20})$ has been titrated with the fluoroquinolone ciprofloxacin (CFX) using ^1H 1D and 2D NMR spectroscopy to monitor the interaction pattern. The assignments of key intermolecular proton–proton crosspeaks in the NOESY map between the fluoroquinolone and the duplex prove the existence of predominantly minor groove CFX–duplex interactions. When $MgCl_2$ was added to a solution of 1:1 CFX–duplex until a final concentration of Mg^{2+}–$[PO_4] = 1$, the binding pattern did not change significantly. Theoretical calculations (Docking) carried out on a model of the ternary CFX–Mg^{2+}–duplex adduct using a key interproton distance derived from the NOESY map as anchoring, produced an energetically favourable orientation of the CFX–Mg^{2+} in the minor groove.

Keywords: Ciprofloxacin; Fluoroquinolone; Ligand–DNA interactions; NMR; Docking

1. Introduction

Quinolones are an important group of antibiotics and several quinolones are in common clinical use. The first quinolone antibiotic, nalidixic acid, was synthesized in 1962 by Lesher et al. [1]. Ciprofloxacin (CFX) (Scheme 1), a typical second-generation fluoroquinolone, has been in clinical use for more than a decade and sold for $US 1.5 billion in 1996 [2]. The drug has been the centre of great interest and success and over 15 000 articles have been published about ciprofloxacin. Quite recently, in connection with the outbreak of suspected anthrax biological warfare, many experts consider ciprofloxacin the drug of choice for treating victims. Resistance against antibiotics is on the rise and multi-drug resistance will probably become a major problem in the 21st century. It is therefore vital to gather knowledge about the molecular mechanisms of action for antibiotics.

As all quinolones, ciprofloxacin is active against the DNA gyrase enzyme, a type II topoisomerase. DNA gyrase introduce negative supercoils in DNA [3] by wrapping the DNA around the enzyme. The enzyme then catalyzes the breakage of a segment of the wrapped DNA, the passage of a segment of the same DNA through the break and finally the religation of the break [4]. In this way, DNA 'knots' are resolved and the DNA is exposed for replication processes.

The enzyme is essential for all bacteria and is therefore an excellent target for antibiotics. Quinolones turn the action of gyrase against the bacteria by blocking the strand passage and thereby hindering proper replication of DNA. This eventually leads to cell death. Currently several structural models have been suggested to account for the action of quinolones. They all require a direct interaction between the drug and either single-or double-stranded DNA [5–7]. One of the more recent models also suggests that Mg^{2+} plays an important role in the drug binding to a DNA–gyrase complex [7–10]. It was reported that a reasonably strong interaction between quinolones and plasmid or single-stranded DNA occurs only in the presence of physiological concentration of Mg^{2+} [7]. A good relationship was

* Corresponding author. Tel.: +47-555-83 352; fax: +47-555-89 490.
E-mail address: einar.sletten@kj.uib.no (E. Sletten).

0020-1693/02/$ - see front matter
PII: S0020-1693(02)00933-7

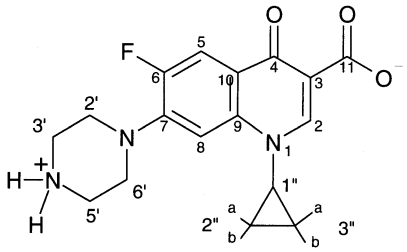

Scheme 1. Structure of ciprofloxacin in the zwitterionic form. 'a' and 'b' designate protons *trans* and *cis* to the H1″ proton, respectively.

found between the binding constants for the ternary DNA–drug–Mg^{2+} complex (K_T) and gyrase poisoning activity. The authors did not suggest a structural model for the ternary complex, except reporting that the data did not support a mechanism of action based upon quinolone intercalation into B-DNA [11]. This conclusion is in agreement with results based on CD and LD measurements of a calf thymus DNA–norfloxacin system where the drug chromophore is significantly tilted with respect to the DNA axis [12]. On the contrary, Nordén et al. [13] using similar experimental methods found a near perpendicular orientation of the norfloxacin chromophore plane relative to the DNA axis that excludes classical groove or surface binding. However, the possibility of classical intercalation was ruled out based on DNA unwinding experiments. The equilibrium constant of the norfloxacin–DNA complex formation was estimated at 2.8×10^3 M^{-1} at 25 °C [13].

Several questions still remain to be answered regarding quinolone-DNA interactions: (i) preference for single-or double-stranded DNA binding; (ii) the role of Mg^{2+} ions; (iii) groove binding versus classical intercalation. Here, we present results aimed towards giving better insight into the structure of the complex between fluoroquinolone and double stranded DNA. A DNA model system represented by a double-helical 10 base pair oligonucleotide was employed to form adducts with ciprofloxacin. We report ^{1}H NMR results obtained for the ciprofloxacin-oligonucleotide solution without and in the presence of Mg^{2+} ions.

2. Experimental

2.1. Sample preparation

The decamer 5′-d($C_1C_2T_3C_4G_5C_6T_7C_8T_9C_{10}$)·d($G_{11}A_{12}G_{13}A_{14}G_{15}C_{16}G_{17}A_{18}G_{19}G_{20}$)-3′ was purchased from Oswell DNA Service as a gel purified compound. The sample needed further purification and was run through a Dowex Ion-Exchange column, a Sephadex G-25 desalting column and finally a Chelex column for removal of paramagnetic impurities. The sample was then dissolved in 90% H_2O–10% D_2O, 100 mM NaCl was added to the solution and pH was regulated to 5.9. No buffer was used in these experiments. Control measurements before and after Mg^{2+}-titration showed pH variations within experimental error (±0.05 pH). The duplex concentration was 1.5 mM throughout the experiments. The second set of experiments was run in pure D_2O, 99.96% quality from Fluorochem Limited. CFX was obtained from ICN Pharmaceuticals in solid state as CFX·HCl·H_2O and used without further purification.

2.2. NMR measurements

The ^{1}H NMR spectra were recorded on a Bruker DRX 600 spectrometer operating at a field of 14.1 Tesla, $T = 298$ K. The chemical shifts were referred to the water signal at 4.76 ppm, 298 K. The 2D NOESY spectra were recorded with mixing times between 200 and 300 ms. A total of 512 t_1 increments, each with 2048 t_2 complex points, were collected with each FID as the average of 32–80 transients. In the t_1 dimension, linear prediction and zero filling was applied to reach a size of 2048 data points, as in the t_2 dimension. For resolution enhancement, a Gaussian apodization function with line broadening of −3 to 0.0 Hz (−15.0 Hz in the t_1 dimension) and Gaussian broadening of 0.15 was used in both dimensions. For distance determination purposes, the 2D spectra were also processed with a 90° phase-shifted, squared sine bell apodization function in both dimensions. A line broadening of 0.3 Hz was applied. For the first series, successive aliquots of 15.0 mM ciprofloxacin were added up to a 1:1 CFX–DNA ratio. For the second series successive aliquots of 900 mM $MgCl_2$ was added up to 20:1 Mg^{2+}–DNA. The magnesium titration experiment was performed with D_2O as solvent instead of water. D_2O was chosen to gain better resolution by having a narrower spectral region and thereby increasing the number of data points per frequency unit and simplifying the spectra by removing the signals from exchangeable protons which disappear from the spectra due to exchange with deuterium. NMR processing was performed using XWIN-NMR (Bruker), SPARKY [14] and MESTRE-C 2.3a [15] software.

2.3. Docking experiments

The docking experiments were carried out using the DOCK 4.0.1 suite of programs [16]. A model of the CFX–Mg^{2+} complex was obtained by energy minimization using a modified Amber forcefield. The 10-mer duplex structure was built as standard B-form DNA using InsightII (Biosym Ltd.). Clusters were generated within a box with dimensions $18.0 \times 18.0 \times 18.0$ Å, enclosing the base-pairs C4-G17 toT9-A12. A grid calculation was performed with grid spacing 0.10 Å

and a classic 6–12 Lennard–Jones energy potential was used for the energy calculations during the docking process. A linear distance-dependent dielectric constant was used. Between 5000 and 50 000 orientations were scored for electrostatic and van der Waals interactions. Of the 30 lowest energy-scoring orientations, a minor groove binder of suitable orientation was selected as input for further docking refinement. In this next step the cyclopropyl and piperazine rings on CFX were allowed free rotation. Subsequently, the orientation closest resembling the NMR derived connectivities was selected as input for the final docking where CFX was anchored by fixing the distances between the piperazine proton H5′ and the duplex proton A14 H1′. The results were visualized using the CHIMERA [17] and VMD [18] software.

3. Results and discussion

3.1. Ciprofloxacin and DNA

The 1D ^{1}H NMR spectra recorded for the CFX titration of the oligonucleotide 5′-d($C_1C_2T_3C_4G_5C_6T_7C_8T_9C_{10}$) · d($G_{11}A_{12}G_{13}A_{14}G_{15}C_{16}G_{17}A_{18}G_{19}G_{20}$)-3′ are shown in Fig. 1. The addition of CFX induces a general broadening of all peaks. However, one may notice an additional selective broadening of some signals. The intensities of the G5, G13, G15, and G17 H8 signals are dramatically reduced upon ciprofloxacin addition, while H8 of the 'end-guanines' G11, G19 and G20 are much less affected. Other signals showing

Table 1
^{1}H NMR linewidths at half-height for selected signals in the 1D spectra

r (CFX–DNA)		0 [a]	0.19	0.38
	A12	6.1	7.1	10.1
	A18	7.6	8.3	11.7
	A14	6.4	10.0	14.1
H8	G5	7.2	11.6	20.3
	G17	8.6	12.5	
	G11	8.0	8.2	12.8
	T9	5.0	6.0	7.1
CH3	T3	5.2	6.6	8.3
	T7	5.3	8.7	12.4

Above $r(n_{CFX}:n_{duplex}) = 0.38$, the general line broadening prevents acceptable measurements for the H8 protons. The methyl proton linebroadening follow the same trend up to $r = 0.96$.

[a] All linewidths in Hz.

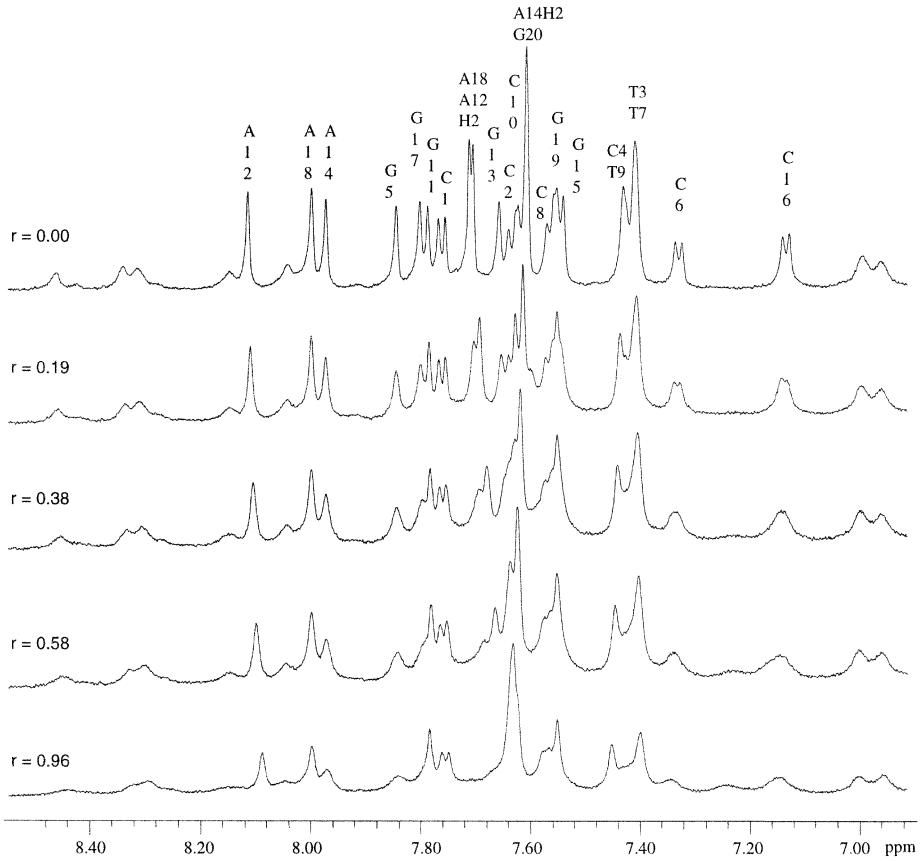

Fig. 1. ^{1}H NMR (600 MHz) spectra at 298 K of the low-field region of the duplex form of d($C_1C_2T_3C_4G_5C_6T_7C_8T_9C_{10}$)·d($G_{11}A_{12}G_{13}A_{14}G_{15}C_{16}$-$G_{17}A_{18}G_{19}G_{20}$). The duplex was dissolved in 90% H_2O–10% D_2O, 0.1 M NaCl, pH 5.9. Successive amounts of CFX were added to a final molar ratio $r = 0.96$ (n_{CFX}–n_{duplex}). Labels C1-G20 refer to H8/H6 protons for purine–pyrimidines. Non-labeled peaks are amino protons.

pronounced line broadening are A14 H8 and the T7 CH3 (Table 1). The largest chemical shifts induced by CFX are experienced by adenine H2 protons (0.03–0.07 ppm) (Table S1). Other small but significant chemical shifts of aromatic protons are observed for A12 H8 (−0.03 ppm) and T9 H6 (+0.02 ppm).

NOESY spectra were recorded at 0:1, 0.6:1 and 1:1 drug–DNA ratios. In Fig. 2, the aromatic–anomeric region of the NOESY spectrum at 1:1 ratio, a complete sequential walk is depicted. The relative intensities of the crosspeaks in this region are comparable to those of the native duplex indicating that CFX does not destroy the B-form duplex geometry. A close examination of the aromatic/aromatic region (data not shown) does not reveal any signs of classical intercalation between CFX and the duplex. Significant changes in the spectrum at 1:1 ratio are the decrease of intensity of the C16 N4H1 crosspeaks to C16 N4H2 and C4 N4H1 to C4 N4H2. For G13, both the H8 (−0.03) and the H1′ (−0.04) signals have shifted upfield. A14 H1′ (−0.04) has shifted upfield. T9 H6 (+0.02) has shifted downfield, while T7 H6 (−0.01) and T3 H6 (−0.01) have shifted upfield.

The Watson–Crick base-pairs are still intact in the solution of 1:1 CFX–duplex as demonstrated by the positions of the guanine and thymine imino proton resonances (data not shown). The most dramatic changes in the imino region are shown in the NOESY map (Fig. 3(a) and (b)) where the crosspeak between the solvent exposed amino proton C16 N4H2 and the imino proton G5 N1H has vanished. A similar situation is observed for the neighboring central base pair C6 N4H2-G15 N1H. This indicates that the addition of ciprofloxacin does influence the hydration of the B-form duplex through minor or major groove interaction.

The most important results obtained from the NOESY titration experiment are the presence of several significant crosspeaks between ciprofloxacin protons and the duplex. However, due to severe overlap some key crosspeak assignments involving CFX H2, H5, and H8 and the duplex protons could not be made with certainty. Fortunately, a clear chemical shift region for the crosspeaks involving piperazine protons and anomeric H1′ protons enable us to unambiguously confirm true intermolecular contacts between CFX and the duplex (Fig. 4(a) and (b)).

The crosspeaks to the anomeric protons of T3, T7 and C8 are strongest, and weaker crosspeaks are observed to their neighboring bases, indicating that CFX does experience some flexibility in the duplex interaction. The crosspeak intensities correspond to distances of 3.0–4.5 Å between anomeric and piperazine protons and the crosspeaks are consistent with CFX interaction in

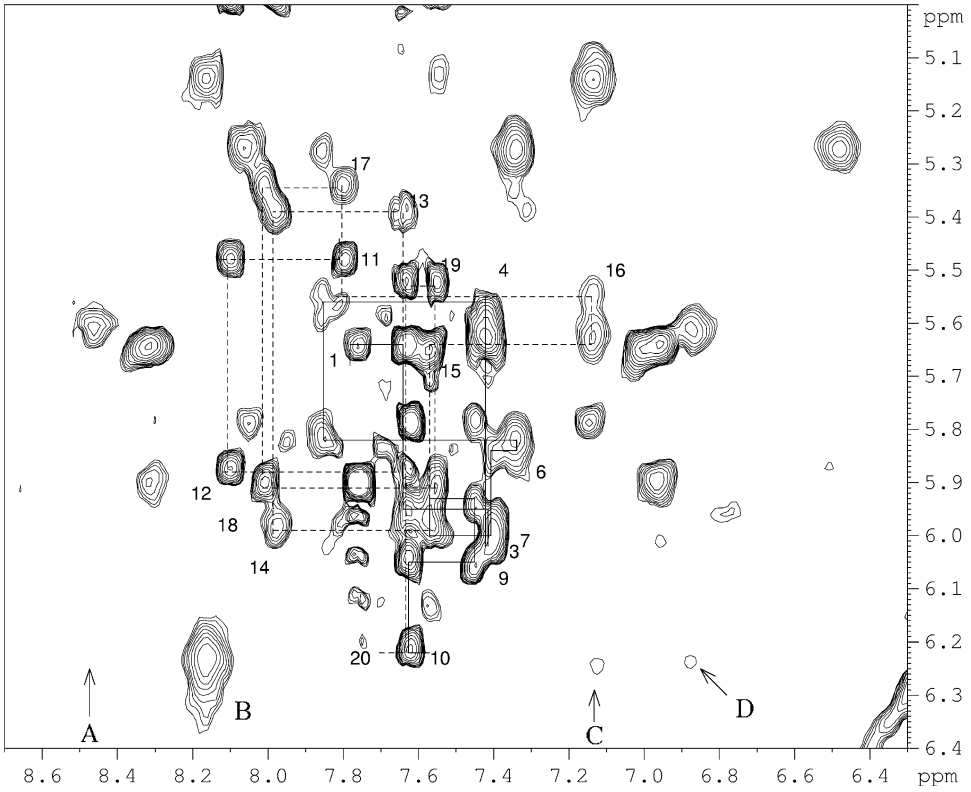

Fig. 2. Contour plot of one region of the 600 MHz NOESY spectrum of a sample containing the duplex $d(C_1C_2T_3C_4G_5C_6T_7C_8T_9C_{10})\cdot d(G_{11}A_{12}G_{13}A_{14}G_{15}C_{16}G_{17}A_{18}G_{19}G_{20})$ and CFX in 1:1 molar ratio. The sequential connectivities are indicated with solid and broken lines for the two strands, respectively. The mixing time was 200 ms and the temperature 298. The four crosspeaks denoted by letters are: (A) C4 N4H1–C16 N4H2, (B) C16 N4H1–N4H2, (C) C16 H6–N4H2 and (D) C4 N4H2–C16 N4H2.

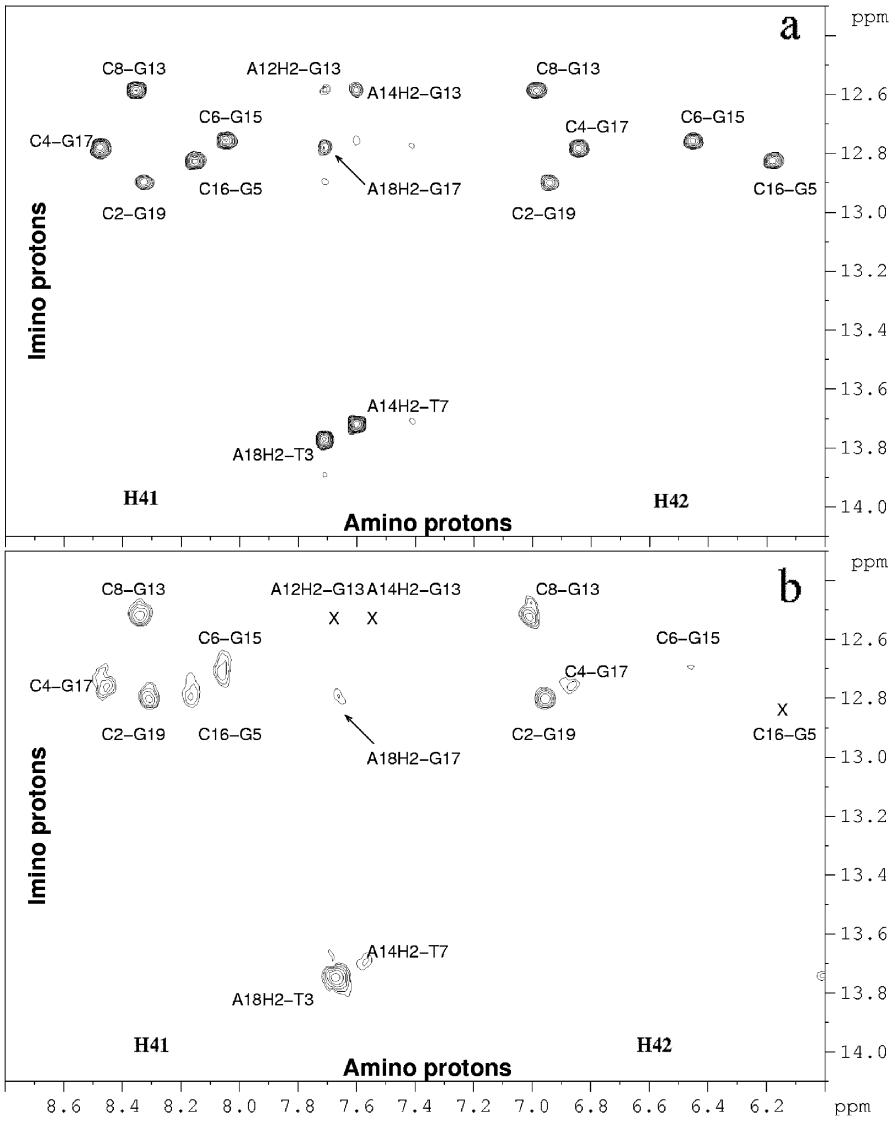

Fig. 3. Contour plots of the aromatic-imino region; (a) native duplex, (b) 1:1 CFX–duplex (corresponding to Fig. 2).

the minor groove. This kind of detailed structural information on the binding of fluoroquinolones to DNA is previously unreported. A summary of the observed crosspeaks representing intermolecular contacts is listed in Table 2.

3.2. Ciprofloxacin–Mg^{2+}–DNA interaction

The 1:1 CFX–DNA solution (CFX–[PO_4] ratio = 1:20) was titrated with $MgCl_2$ over a wide range of concentrations covering both the low physiological 'free' concentration of Mg^{2+} (1–2 mM) [19] and the upper range of 30 mM corresponding to Mg^{2+}–[PO_4] ≈ 1. The molar ratio of the final ternary mixture Mg^{2+}–CFX–duplex was 20:1:1. The deprotonated carboxyl group ($pK_{a1} = 6.1$) [20] is the obvious target for metal ion as recognized in several reports [21–25]. The binding constant for Mg^{2+} to CFX is reported to be $1.30 \pm 0.05 \times 10^3$ M^{-1} [8]. As a comparison, the binding constant of Mg^{2+}–DNA (pBR322) is $22 \pm 4 \times 10^3$ M^{-1} [7]. The 2D spectra show that CFX H2 shifts downfield from 8.23 to 8.43 ppm (Table 2). This shift can be explained by the chelation of the keto-carboxyl group by Mg^{2+}. The binding site can be made even more attractive to metal ions by envisaging a type of keto-enol tautomerism similar to the classic carbonyl α-substitution reaction. The enol character will induce a positive charge on C2 and C5 and this will result in a deshielding of the H2 and H5 protons, leading to downfield shifts. A similar mechanism may explain the downfield shift (0.48 ppm) observed for CFX H2 in the chelate of CFX–Al^{3+} [26]. In this Al-chelate at pH 2.5

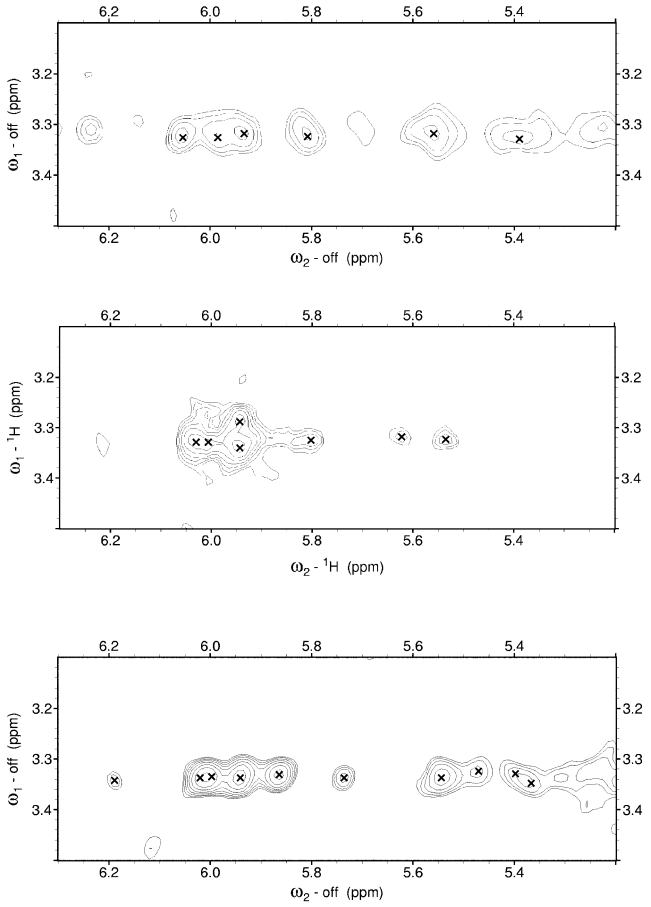

Fig. 4. Contour plots of the ^{1}H crosspeaks between the piperazine moiety and the anomeric protons of the duplex; (top) CFX–duplex 0.6:1; (middle) CFX–duplex 1:1; (bottom) Mg^{2+}–CFX–duplex 20:1:1.

the downfield shift is about twice as large as the one observed with magnesium. The smaller change in chemical shift seems reasonable considering the lower charge of Mg^{2+} as compared with Al^{3+}. In addition, at pH 2.5 the carboxyl group has to first be deprotonated before chelation can occur, while in our system, at pH 5.9, the carboxyl group is partly deprotonated.

Based on ^{19}F NMR studies Lecomte et al. [8] suggest Mg^{2+} binding involving first the carbonyl and carboxylate groups, then the N4′ piperazinyl atom. Our results for the ternary CFX–Mg^{2+}–duplex do not support this conclusion. Mg^{2+}-binding to the N4′ atom would induce a strong deshielding of the H(3′, 5′) protons, producing a significant downfield shift of these protons. Even at the Mg^{2+}–CFX ratio of 20:1 there is no sign of this strong deshielding indicating that N4′ is not bound to Mg^{2+} at his molar ratio. The overlapping piperazine signals H(2′, 6′) and H(3′, 5′) at 3.33 ppm are partly separated at $r = 20.08$. This observation could indicate that there is a stabilization of one (or several) species with hindered rotation around the piperazinyl bond. In the crystal structure of the CFX–Mg^{2+} complex a short distance (2.28 Å) [27] between the fluor substituents and one of the piperazine ring protons may be characterized as a C–H···F hydrogen bond. Fixing the piperazine conformation by introducing a fluor substituent on the quinolone ring may be of importance for fitting CFX in the minor groove and consequently, relevant for the improved efficacy of fluoroquinolones as antibacterial agents.

Interestingly, the addition of Mg^{2+} does not seem to change the predominant CFX–duplex interaction mode. On the contrary, the binding in the minor groove seems to be further stabilized. The addition of Mg^{2+} induces a general line broadening and weakening of signals, but still the piperazine-duplex crosspeaks are stronger than in the absence of Mg^{2+}. As seen in Fig. 4(c), there are four strong crosspeaks between the piperazine protons and the anomeric proton of the neighboring bases: C8, T9, A12 and A14. Weak crosspeaks to anomeric protons of adjacent bases are also observed, as for the titration without Mg^{2+}. Ambiguous assignments due to the crowdedness of the anomeric region of the NMR spectrum prevent speculation of sequence specificity in the mode of interaction between CFX and the duplex. The minor groove is narrow and electrostatic interactions between the negatively charged keto-carboxyl moiety and the negatively charged phosphate backbone will severely destabilize any interaction in this region. In principle, the +2 charge of the CFX-Mg^{2+} complex should make it a better candidate for groove binding, thus the increased affinity for the duplex seems reasonable. Mg^{2+}-ions are shown to interact with both the minor and the major groove of DNA [28,29] and are known as good counterions for stabilizing the duplex DNA because of a beneficial relation between effective charge and ionic radius [30].

In the 2D NOESY spectrum of CFX–Mg^{2+} (data not shown), intramolecular crosspeaks are observed between all substituents of ciprofloxacin except for CFX H5, which is broad with low intensity. A double set of resonances for the cyclopropyl H(2″a, 3″a) and H(2″b, 3″b) protons are observed. The resonances are shifted −0.08 and −0.07, respectively. The second set of resonances has low intensity and is probably related to a different cyclopropyl conformation. In the dominating conformation, the cyclopropyl ring is tilted with respect to the aromatic plane so that the CFX H1″ proton is on average closer to CFX H8 than CFX H2. This is seen from integration of intramolecular cyclopropyl proton crosspeaks with H8 and H2. In the interaction with the duplex, the cyclopropyl ring is thought to point out of the minor groove, as it has no significant crosspeaks to the duplex.

CFX is relatively insoluble in water at or near physiological pH. The zwitterionic character due to the carboxylic group ($pK_{a1} = 6.1$) and the imino proton ($pK_{a2} = 8.7$) [20] is expected to enhance the tendency to

Table 2
Intermolecular NOE crosspeaks between ciprofloxacin and the d($C_1C_2T_3C_4G_5C_6T_7C_8T_9C_{10}$)·d($G_{11}A_{12}G_{13}A_{14}G_{15}C_{16}G_{17}A_{18}G_{19}G_{20}$) duplex at different concentration levels of CFX and Mg^{2+}

CFX proton(s)	Chemical shift [a]	Crosspeaks to 5′-d(CCTCGCTCTC)·d(GAGAGCGAGG)-3′ at different Mg^{2+}–CFX–DNA ratios [b]
CFX H2	8.23	–
	8.29	G5 H8(vw), T7 H2″(vw), C8 N4H1(vw), C10 H5(vw), G13 H2′(vw), G15 H2″(vw)
	8.43	–
CFX H8	7.22	G5 H1′(vw), T7 CH3(vw), G11 H8(w), G15 H8(w), G20 H8(m)
	7.22	G11 H8(vw), G15 H8(vw), G20 H8(w)
	7.25	–
CFX H(2′, 6′)	3.36	C16 N4H2(vw)
	3.37	C2 H6(m), C6 H4′(vw), C8 N4H1(vw), A14 H2′(vw), G19 H2′(w)
	3.35	–
CFX H(2′, 6′), H(3′, 5′) [c]	3.33	C2 H2″(w), C4 H1′(w), G5 H1′(w), T7 H1′(w), C8 H1′(w), T9 H1′(w), G13 H1′(w), G15 H2″(w), C16 H6(w)
	3.33	C2 H1′(m), G5 H1′/C10 H5(w), C6 H1′(w), T7 H1′(m), C8 H1′(m), G15 H1′ (vw), G19 H1′(w)
	3.34	C1 H5(w), C2 H1′(vw), C8 H1′(s), C8 H2″(vw), T9 H1′(s), C10 H1′(vw), C10 H5(w), G11 H1′(w), A12 H1′(s), G13 H1′(w), A14 H1′(s), C16 H1′(m), G17 H1′(w), G20 H8(m)
CFX H(3′, 5′)	3.32	–
	3.29	T3 H1′(m), C8H1′(m), C8 H2″(m) G13 H8(w), G20 H8(m)
	3.32	–
CFX H(2″b, 3″b)	1.21	C16 N4H1(vw)
	1.22	C2 H1′(w), C6 H4′(w), A12 H1′(vw), A12 H2″(vw), A14 H1′(w), G19 H1′(vw)
	1.17	T9 H3′(vw), C16 H1′(vw)
CFX H(2″a, 3″a)	0.95	C2 H2″(vw), A12 H1′(vw), C16 H1′(vw), C16 N4H1(vw)
	0.95	C2 H1′(w), C2 H3′(w), C6 H4′(vw), T7 H2″(w), A12 H1′(w), A12 H8(vw)
	0.90	A12 H1′(vw), C16 H1′(vw)

Ambiguous assignments are designated by '/'.
[a] The concentration ratios (Mg^{2+}–CFX–DNA) in the table are (top) 0:0.6:1, (middle) 0:1:1 and (bottom) 20:1:1.
[b] Crosspeak intensities are reported as vs = very strong, s = strong, m = medium, w = weak and vw = very weak, referenced to the C6 H5-H6 crosspeak (vs).
[c] The CFX H(2′, 6′),H(3′, 5′) resonance corresponds to the coalescence of the two piperazine resonances CFX H(2′, 6′) and H(3′, 5′).

form head-to-tail stacking, a phenomena elegantly described by Sigel et al. for nucleic acid components [31]. In the NOESY map unexpected small but significant crosspeaks are observed between CFX H5 and propyl protons. Since the corresponding distance is too long to produce intramolecular NOE effects one may have to invoke some kind of dipolar CFX–CFX stacking interaction enhanced through groove binding in the duplex.

3.3. Docking results

The docking experiments were performed to gain further insight into the structure of the interaction between ciprofloxacin and DNA in the presence of Mg^{2+}. The results of docking the CFX–Mg^{2+}-complex, starting from a random orientation, showed that minor and major groove binding is energetically similar (Fig. 5). Following a second docking with a minor groove binder, CFX was anchored in the minor groove by fixing the distance A14 H1′–CFX H6′ at 3.3 Å (derived from the NOESY data). The minimization process produced a best orientation with energy score lower than the best result for the non-anchored groove orientations (Fig. 6). The contacts depicted in Fig. 6 are in qualitative agreement with the distances derived from the 2D NOESY spectra. The docked ciprofloxacin has several NOE contacts < 5 Å between the aromatic CFX protons and protons of the duplex. Many of the corresponding crosspeaks are too weak to be detected in the NMR spectra and can therefore not give further insight into the validity of the suggested model. The Mg^{2+}-ion is located close to the solvent-exposed O2 of the thymine base and to the O4′ of the phosphate groups, with possibilities for both direct and ligand mediated interactions. An important contribution to the stabilizing electrostatic interactions is the almost perfect complementary shape of the minor groove for the CFX–Mg^{2+} complex.

4. Conclusion

The crosspeaks between the piperazine moiety of ciprofloxacin and the anomeric protons of the 10-mer duplex show that the drug is located predominantly in the minor groove both without and in the presence of Mg^{2+}-ions. The non-restrained docking calculations do not distinguish between minor and major groove binding. However, docking in combination with experimental distance restraints produce a geometry which is energetically favorable. It is clear from the data pre-

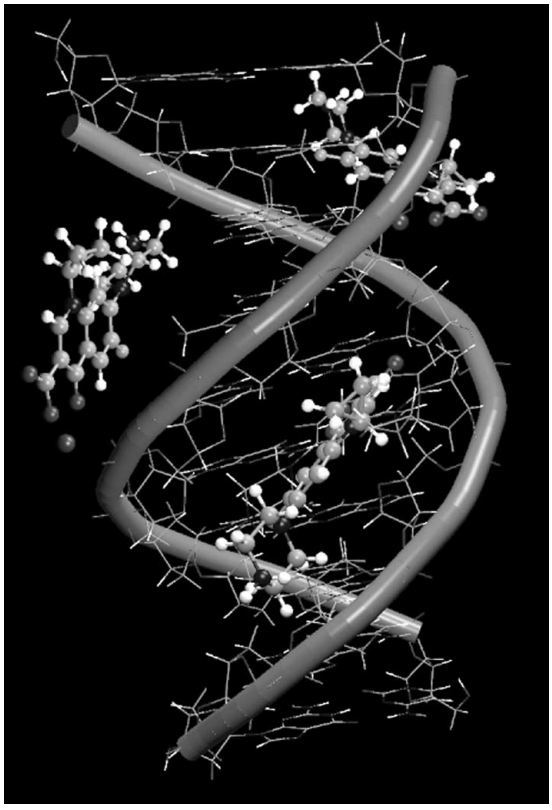

Fig. 5. Docking results for the first screening of possible binding orientations. The orientations represent three major groups of orientations. The upper right orientation constituted about 25% of the 50 lowest energy scoring orientations. The orientation shown has the lowest energy (-43.7 kcal mol^{-1}) of all orientations. The middle minor groove orientation was higher in energy (-40.4 kcal mol^{-1}) and the population of this group was similar to the upper minor groove orientation. The largest group was the major groove binder, constituting about 50% of the 50 lowest energy scoring orientations. The major groove binders were in general higher in energy than the minor groove binders, although the orientation in Fig. 5 had particularly low energy, -43.05 kcal mol^{-1}. The duplex is depicted with positive z-axis parallel to the duplex helix axis in the 5′–3′ direction of the C1–C10 strand.

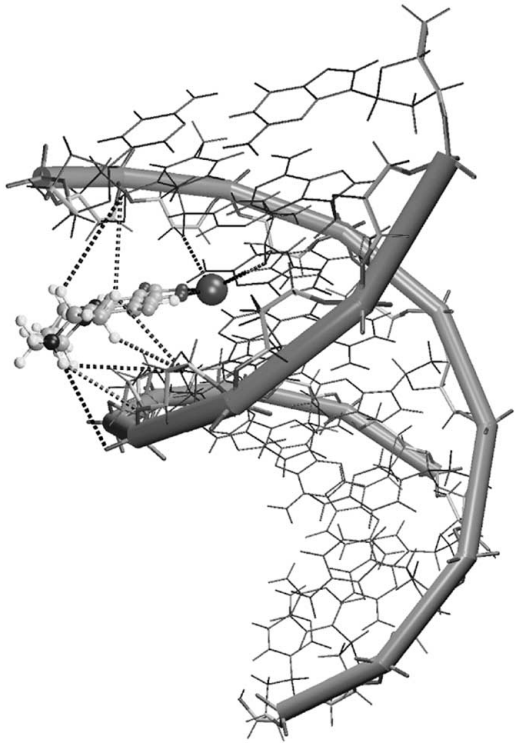

Fig. 6. The CFX–Mg^{2+} complex was anchored in the minor groove of the duplex. The anchored docking returned 12 orientations, where the depicted orientation had the third lowest energy. The energies of the lowest scoring orientations were 7–12 kcal mol^{-1} lower than the best orientations from the first docking. The orientations differed only in the rotation of the piperazine and the cyclopropyl rings. Indicated by dotted lines are observed NOE contacts and possible electrostatic stabilizing factors. The following NOE contacts are shown: CFX $H6'_{ax.}$–A14 H1′ (3.3 Å, anchored), CFX $H6'_{eq.}$–A14 H1′ (4.4 Å), CFX $H6'_{eq.}$–T9 H1′ (4.2 Å) and CFX $H5'_{ax.}$–T9 H1′ (4.8 Å). The distances are in agreement with the observed crosspeak intensities in the NOESY spectra. Also shown are possible electrostatic interactions: CFX $N4'H_{ax.}$–A14 O3′ (3.6 Å), CFX $N4'H_{ax.}$–G15 OP1 (4.3 Å), Mg–T7 O4′ (3.5 Å), Mg–T7 O2 (2.3 Å) and Mg–C8 O4′ (3.0 Å). The duplex is depicted with positive z-axis parallel to the duplex helix axis in the 5′–3′ direction of the C1–C10 strand. Therefore, T9 H1′ is located directly above CFX, while A14 H1′ is situated directly below.

sented that classic intercalation between ciprofloxacin and the duplex must be ruled out. The present results are obtained on a relatively small model system (10-mer duplex) and may not be directly comparable to previous studies on quinolone binding to e.g. herring sperm DNA or supercoiled plasmids. We are now planning to use longer oligonucleotides as model system in order to investigate potential sequence-selective binding of fluoroquinolones to DNA. The ability of ciprofloxacin in the zwitterionic form to engage in self-stacking will be investigated further.

5. Supplementary material

1D ^{1}H NMR spectrum of the imino region of 1:1 CFX–Duplex. ^{1}H chemical shifts for CFX–duplex–Mg^{2+} ratios: 0:1:0, 0.6:1:0, 1:1:0, 1:1.20. Available from the authors on request.

Acknowledgements

This work was supported by The Norwegian Research Council (135055/432) and (145183/432) and the COST D20 Action. Computer time on SGI Octane at the Department of Biochemistry, University of Bergen is gratefully acknowledged.

References

[1] G.Y. Lesher, E.D. Forelich, M.D. Gruet, J.H. Bailey, R.P. Brundage, J. Med. Pharm. Chem. 5 (1962) 1063.

[2] S.L. Gorbach, K.W. Nelson, in: A.P.R. Wilson, R.N. Grüneberg (Eds.), Ciprofloxacin: 10 Years of Clinical Experience, Maxim Medical, Oxford, 1997, p. 1.
[3] M. Gellert, K. Mizuuchi, M.H. O'Dea, H.A. Nash, Proc. Natl. Acad. Sci. USA 73 (1976) 3872.
[4] L.L. Shen, D.T.W. Chu, Cur. Pharm. Des. 2 (1996) 195.
[5] L.L. Shen, A.G. Pernet, Proc. Natl. Acad. Sci. USA 82 (1985) 307.
[6] S.C. Kampranis, A. Maxwell, J. Biol. Chem. 273 (1998) 22615.
[7] G. Palú, S. Valisena, G. Ciarrocchi, B. Gatto, M. Palumbo, Proc. Natl. Acad. Sci. USA 89 (1992) 9671.
[8] S. Lecomte, M.H. Baron, M.T. Chenon, C. Coupry, N.J. Moreau, Antimicrob. Agents Chemother. 38 (1994) 2810.
[9] S. Lecomte, N.J. Moreau, M.-T. Chenon, Int. J. Pharm. 164 (1998) 57.
[10] J.Y. Fan, D. Sun, H.T. Yu, S.M. Kerwin, L.H. Hurley, J. Med. Chem. 38 (1995) 408.
[11] C. Sissi, M. Andreolli, V. Cecchetti, A. Fravolini, B. Gatto, M. Palumbo, Bioorg. Med. Chem. 6 (1998) 1555.
[12] C. Bailly, P. Colson, C. Houssier, Biochem. Biophys. Res. Commun. 243 (1998) 844.
[13] G.S. Son, J.-A. Yeo, M.-S. Kim, S.K. Kim, A. Holmén, B. Åkerman, B. Nordén, J. Am. Chem. Soc. 120 (1998) 6451.
[14] T.D. Goddard, D.G. Kneller, SPARKY 3, University of California, San Francisco.
[15] C. Cobas, J. Cruces, F.J. Sardina, MESTREC 2.3, Universidad de Santiago de Compostela, Spain.
[16] T.J.A. Ewing, I.D. Kuntz, J. Comput. Chem. 18 (1997) 1175.
[17] C.C. Huang, G.S. Couch, E.F. Pettersen, T.E. Ferrin, Pacific Symp. Biocomp. 1 (1996) 724.
[18] W. Humphrey, A. Dalke, K. Schulten, J. Molec. Graphics 14 (1996) 33.
[19] M.D. Snavely, in: H. Sigel (Ed.), Metal Ions in Biological Systems, vol. 26, Marcel Dekker, New York, 1990, pp. 155–175.
[20] Y.X. Furet, J. Deshusses, J.C. Pechere, Animicrob. Agents Chemother. 36 (1992) 2506.
[21] J.H. Morais Cabral, A.P. Jackson, C.V. Smith, N. Shikotra, A. Maxwell, R.C. Liddington, Nature 388 (1997) 903.
[22] F. Sörgel, M. Kinzig, Am. J. Med. 94 (1993) 44S.
[23] C.M. Riley, C.G. Kindberg, V.J. Stella, in: P.B. Fernandes (Ed.), International Telesymposium on Quinolones, Prous Science Publishers, Barcelona, 1989, pp. 21–36.
[24] J. Hernàndez-Borrell, M.T. Montero, J. Chem. Educ. 74 (1997) 1311.
[25] A. Bauernfeind, C. Petermuller, Eur. J. Clin. Microbiol. 2 (1983) 111.
[26] M. Sakai, A. Hara, S. Anjo, M. Nakamura, J. Pharm. Biomed. Anal. 18 (1999) 1057.
[27] I. Turel, I. Leban, M. Zupancic, P. Bukovec, K. Gruber, Acta Crystallogr. C52 (1996) 2443.
[28] T.K. Chiu, R. Dickerson, J. Mol. Biol. 301 (2000) 915.
[29] G. Minasov, V. Tereshko, M. Egli, J. Mol. Biol. 291 (1999) 83.
[30] C. Klevickis, C.M. Grisham, in: H. Sigel (Ed.), Metal Ions in Biological Systems, vol. 32, Marcel Dekker, New York, 1996, p. 1.
[31] O. Yamauchi, A. Odani, H. Masuda, H. Sigel, in: H. Sigel (Ed.), Metal Ions in Biological Systems, vol. 32, Marcel Dekker, New York, 1996, pp. 207–270.

Supplementary material

Interaction between ciprofloxacin and DNA mediated by Mg^{2+}-ions

T. Skauge[a], I. Turel[b], E. Sletten[a,*]

Table S1. ^{1}H NMR chemical shifts of the duplex, 5′-d($C_1C_2T_3C_4G_5C_6T_7C_8T_9C_{10}$)•d($G_{11}A_{12}G_{13}A_{14}G_{15}C_{16}G_{17}A_{18}G_{19}G_{20}$)-3′ at different concentration levels of ciprofloxacin and Mg^{2+}. The first number in each cell is the chemical shift of the native duplex protons without ciprofloxacin or Mg^{2+}. The second, third and fourth number show the change of chemical shift as compared to that of the native duplex for Mg^{2+}:CFX:DNA ratios 0:0.6:1, 0:1:1 and 20:1:1, respectively. Shifts in parenthesis, "( )", are assignments with an uncertainty between 0.02 and 0.03 ppm. Assignments with higher uncertainty in the shift values are marked "-".

Nucleic Acid Base	H6/H8	H2/H5/ CH3	H1′	H2′	H2′′	H3′	N1H/ N3H	N4H2	N4H1
C1	7.76 0.00 -0.01 0.00	5.92 -0.01 -0.02 -0.05	5.63 0.01 0.01 0.01	2.21 -0.01 -0.02 0.00	2.50 0.00 0.00 -0.01	4.62 0.02 0.02 0.01		- 6.96 0.00	- 8.33 -0.03
C2	7.63 0.00 0.00 0.02	5.63 0.01 0.01 0.01	5.97 -0.01 -0.02 -0.03	2.14 0.00 0.00 0.02	2.46 0.01 0.00 0.00	4.76 0.01 -0.02 -		6.95 0.00 0.00	8.32 -0.02 -0.02
T3	7.40 -0.01 -0.01 0.03	1.58 0.01 0.01 0.01	(6.03) 0.00 0.00 -0.03	- 2.14 0.01 0.04	- 2.29 0.01 0.03	(4.81) 0.01 - -	13.77 -0.01 -0.03		
C4	7.41 0.00 0.00 0.02	5.61 0.00 0.00 0.00	5.55 0.01 0.01 0.02	2.01 0.01 0.02 0.00	2.34 0.00 -0.01 -0.01	4.80 0.01 0.01 -		6.84 0.02 0.03	8.47 0.00 -0.02
G5	7.84 0.00 0.00 0.03		5.82 0.00 0.00 0.00	2.62 0.00 0.01 0.01	2.62 0.00 0.00 0.01	4.92 0.00 0.00 0.01	12.76 -0.02 -0.04		
C6	7.32 0.01 0.01 0.04	5.26 0.00 0.01 0.02	5.81 0.02 0.03 0.04	2.00 0.01 0.01 0.01	2.43 -0.01 -0.02 -0.01	4.62 0.03 0.05 -		6.45 0.02 0.03	8.04 0.01 0.01
T7	7.40 0.00 -0.01 0.00	1.53 0.02 0.02 0.02	5.98 0.00 0.02 -0.01	2.19 0.00 -0.01 0.00	2.48 0.02 -0.01 0.00	4.81 0.00 0.01 -	13.72 -0.01 -0.03		

C8	7.56 0.01 0.01 0.01	5.62 0.02 0.03 0.01	5.94 0.00 0.00 0.00	2.10 0.01 0.00 0.01	2.45 0.00 0.00 0.00	4.72 0.00 0.01 -		6.99 0.01 0.01	8.35 0.00 -0.02
T9	7.42 0.01 0.02 0.02	1.67 0.01 0.01 -0.01	6.04 0.01 0.01 -0.02	2.14 0.00 0.00 0.00	2.45 0.00 0.01 0.01	4.81 0.01 0.01 0.04	13.90 -0.06 -0.16		
C10	7.59 0.02 0.02 0.00	5.78 0.00 0.00 -0.05	6.21 0.00 -0.01 -0.02	- - 2.14 -	2.22 0.01 0.02 0.01	4.51 0.02 0.02 -		- 7.14 0.00	- 8.31 -0.27
G11	7.79 0.00 0.00 -0.01		5.47 0.00 0.00 0.00	2.39 -0.01 -0.02 -0.03	2.58 0.00 -0.01 -0.01	4.75 0.01 0.01 -	12.90 -0.06 -0.23		
A12	8.11 -0.01 -0.03 -0.01	7.70 -0.04 -0.05 -	5.87 0.00 0.00 0.00	2.68 -0.01 -0.02 -0.02	2.79 0.00 0.00 0.01	4.98 0.00 0.00 0.01			
G13	7.65 -0.01 -0.03 0.01		5.42 -0.02 -0.04 -0.01	2.51 -0.03 -0.02 -0.02	2.64 0.00 -0.01 0.02	(4.95) -0.01 -0.03 -0.01	12.60 -0.05 -0.07		
A14	7.97 0.00 0.00 0.02	7.60 -0.02 0.05 -	6.02 -0.02 -0.04 -0.02	2.55 0.01 0.02 0.01	2.83 -0.02 -0.03 -0.02	4.98 -0.01 0.00 0.02			
G15	7.53 0.01 0.01 0.03		5.63 0.00 -0.01 0.00	2.38 0.00 0.00 0.01	2.54 0.01 -0.01 0.00	4.89 -0.02 -0.01 0.02	12.83 -0.02 -0.03		
C16	7.12 0.01 0.01 0.04	5.12 0.01 0.02 0.03	5.54 0.01 0.01 0.01	1.73 0.03 0.05 0.02	2.20 0.01 0.01 0.01	4.75 0.00 - -		6.18 0.03 0.04	8.15 0.00 0.01
G17	7.80 0.00 0.00 0.01		5.34 0.00 0.00 0.02	2.58 -0.01 -0.02 0.01	2.67 -0.02 -0.02 0.00	4.91 0.00 -0.01 0.01	12.79 -0.01 -0.03		
A18	8.00 0.00 0.00 0.01	7.71 -0.03 -0.03 -	5.92 -0.02 -0.02 0.00	2.54 0.00 0.01 0.01	2.75 0.00 0.00 0.00	4.97 -0.01 - 0.01			
G19	7.54 0.01 0.00 0.01		5.54 -0.01 -0.02 -0.01	2.43 -0.02 -0.01 -0.03	2.57 -0.03 -0.01 -0.02	(4.88) 0.00 0.01 0.01	12.90 -0.06 -0.10		
G20	7.60 0.01 0.02 0.01		6.05 -0.01 - -	2.27 0.02 - 0.04	2.39 -0.01 - 0.01	(4.52) - - -	- - 12.80		

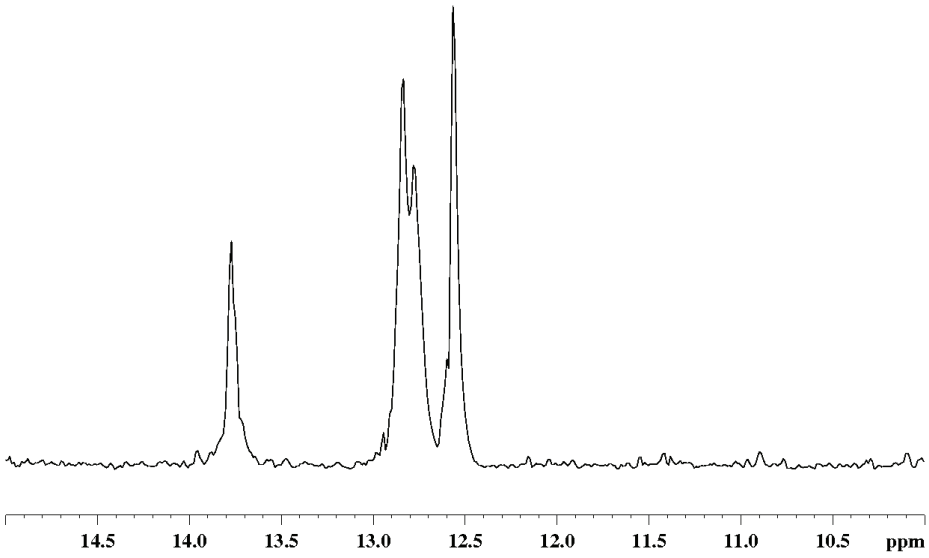

Figure S1. 1D ^{1}H NMR spectrum of the imino region of 1:1 CFX:DNA